



Urban aerosol chemistry at a land–water transition site during summer – Part 1: Impact of agricultural and industrial ammonia emissions

Nicholas Balasus¹, Michael A. Battaglia Jr.¹, Katherine Ball¹, Vanessa Caicedo², Ruben Delgado², Annmarie G. Carlton³, and Christopher J. Hennigan¹

¹Department of Chemical, Biochemical, and Environmental Engineering, University of Maryland, Baltimore County, Baltimore, MD, 21250, USA

²Joint Center for Earth Systems Technology, University of Maryland, Baltimore County, Baltimore, MD, 21250, USA

³Department of Chemistry, University of California, Irvine, CA 92697, USA

Correspondence: Christopher J. Hennigan (hennigan@umbc.edu)

Received: 30 April 2021 – Discussion started: 18 May 2021

Revised: 29 July 2021 – Accepted: 2 August 2021 – Published: 2 September 2021

Abstract. This study characterizes the impact of the Chesapeake Bay and associated meteorological phenomena on aerosol chemistry during the second Ozone Water-Land Environmental Transition Study (OWLETS-2) field campaign, which took place from 4 June to 5 July 2018. Measurements of inorganic PM_{2.5} composition, gas-phase ammonia (NH₃), and an array of meteorological parameters were undertaken at Hart-Miller Island (HMI), a land–water transition site just east of downtown Baltimore on the Chesapeake Bay. The observations at HMI were characterized by abnormally high NH₃ concentrations (maximum of 19.3 μg m⁻³, average of 3.83 μg m⁻³), which were more than a factor of 3 higher than NH₃ levels measured at the closest atmospheric Ammonia Monitoring Network (AMoN) site (approximately 45 km away). While sulfate concentrations at HMI agreed quite well with those measured at a regulatory monitoring station 45 km away, aerosol ammonium and nitrate concentrations were significantly higher, due to the ammonia-rich conditions that resulted from the elevated NH₃. The high NH₃ concentrations were largely due to regional agricultural emissions, including dairy farms in southeastern Pennsylvania and poultry operations in the Delmarva Peninsula (Delaware–Maryland–Virginia). Reduced NH₃ deposition during transport over the Chesapeake Bay likely contributed to enhanced concentrations at HMI compared to the more inland AMoN site. Several peak NH₃ events were recorded, including the maximum NH₃ observed during OWLETS-2, that appear to orig-

inate from a cluster of industrial sources near downtown Baltimore. Such events were all associated with nighttime emissions and advection to HMI under low wind speeds (< 1 m s⁻¹) and stable atmospheric conditions. Our results demonstrate the importance of industrial sources, including several that are not represented in the emissions inventory, on urban air quality. Together with our companion paper, which examines aerosol liquid water and pH during OWLETS-2, we highlight unique processes affecting urban air quality of coastal cities that are distinct from continental locations.

1 Introduction

Inorganic salts, especially sulfate, nitrate, and ammonium, contribute a significant fraction of fine particulate matter (PM_{2.5}) mass in the atmosphere. Ammonia (NH₃) is an important component in this system due to its reaction with acidic species, especially H₂SO₄ (or HSO₄⁻) and HNO₃, to form secondary PM_{2.5}. Volatility differences between H₂SO₄, HNO₃, and NH₃ result in a highly nonlinear system that is strongly influenced by the aerosol liquid water content and by small concentrations of nonvolatile aerosol species (Seinfeld and Pandis, 2016; Guo et al., 2018). The impact of NH₃ on inorganic particulate matter formation has been extensively studied (e.g., Adams et al., 1999; Ansari and Pandis, 1998; Pinder et al., 2008; Bian et al., 2017).

A common finding among these studies, and others, is that the $\text{NH}_3\text{--H}_2\text{SO}_4\text{--HNO}_3\text{--H}_2\text{O}$ system is characterized by “ammonia rich” and “ammonia poor” chemical regimes that produce substantial differences in aerosol composition and mass. These differences have direct implications for aerosol effects on public health (Pozzer et al., 2017; Paulot and Jacob, 2014), nutrient deposition and ecosystem health (Nenes et al., 2021; Bergström and Jansson, 2006), and global climate change (Turnock et al., 2019).

Emissions of the secondary aerosol precursors SO_2 , NO_x , and NH_3 directly affect regional $\text{PM}_{2.5}$ concentrations (Pinder et al., 2007; Zhao et al., 2013). Air quality regulations in the US have substantially decreased SO_2 and NO_x emissions, leading to decreases in ambient $\text{PM}_{2.5}$ (Hand et al., 2012a), while NH_3 has remained largely unregulated. Reductions of NH_3 emissions have been suggested as a cost-effective way to reduce $\text{PM}_{2.5}$, as well (Pinder et al., 2007; Backes et al., 2016). Observations of wet deposition suggest that NH_3 emissions have actually been rising over the past few decades (Keene et al., 2014). Globally, agricultural activity (from livestock and fertilizer application to crops) is the dominant source of NH_3 emissions (Paulot et al., 2015; Pinder et al., 2006; Sutton et al., 2013). Synthetic fertilizer production has recently been identified as an intense local NH_3 source (Van Damme et al., 2018), though its contribution to global emissions is likely small compared to volatilization from synthetic fertilizer applications (Bouwman et al., 1997).

While agriculture collectively emits a dominant fraction of NH_3 globally, numerous other sources contribute to local or regional NH_3 levels, especially in urban areas that are not in close proximity to major agricultural operations. Motor vehicles equipped with catalytic converters can reduce NO to NH_3 in an undesired side reaction, resulting in significant NH_3 emissions (Perrino et al., 2002; Sun et al., 2017; Kean et al., 2009). Anaerobic protein degradation produces NH_3 , as well, resulting in substantial atmospheric emissions from anthropogenic sources present in all urban areas, including landfills, composting, and wastewater treatment (Rittmann and McCarty, 2001; Artíñano et al., 2018). Numerous industrial sources emit NH_3 (Meng et al., 2017), while natural sources (e.g., natural vegetation, wild animals, and large bodies of water) contribute to background NH_3 levels (Paulot et al., 2015; Sutton et al., 2013). Biomass burning also emits NH_3 , though the effects are often seasonal and are most pronounced in regions with intense burning activities (Paulot et al., 2017). In the eastern US, biomass burning intensity is higher in spring and fall than in the summer (Washenfelder et al., 2015).

Urban air quality is controlled by emissions from multiple sectors, meteorology, and dynamic chemical processes that evolve throughout the day. Coastal cities often experience contributions from unique sources (e.g., ocean and shipping emissions), with chemical processes in the polluted marine boundary layer that are distinct from other regions in the atmosphere (e.g., de Gouw et al., 2005; Vutukuru and Dabdub,

2008). Further, meteorological processes associated with the land–water transition can exert a controlling effect on urban air quality that are absent in continental cities. One such phenomenon is the land–sea breeze (or bay breeze), which can prevent or reduce dispersion and contribute to enhanced secondary pollutant formation by recirculating primary urban emissions (Arya, 1999). This contributes to ozone exceedances and increased PM concentrations in highly populated coastal regions (Loughner et al., 2011; Caicedo et al., 2019). Understanding this process is critical since approximately 40 % of the US population lives in “Coastal Shoreline Counties” (NOAA, 2013). The purpose of the National Aeronautics and Space Administration (NASA) and Maryland Department of the Environment (MDE)-sponsored Ozone Water-Land Environmental Transitions Study (OWLETS-2) was to characterize the impacts of the Chesapeake Bay and its associated meteorological phenomena on air pollution formation and transport near Baltimore (Sullivan et al., 2019). In this study, we characterize secondary aerosol formation and sources of elevated NH_3 measured at Hart-Miller Island, MD, a land–water transition site near Baltimore. In the companion paper, we analyze the effects of the Chesapeake Bay and elevated NH_3 on aerosol liquid water content and aerosol pH during OWLETS-2 (Battaglia Jr. et al., 2021).

2 Methods

2.1 Site description

The OWLETS-2 campaign was a field study with multiple measurement platforms coordinating simultaneous water and land measurements of trace gases, aerosols, and meteorological parameters. This study presents analysis of inorganic aerosol composition and gas-phase ammonia measurements made at the Hart-Miller Island (HMI, Fig. 1) supersite. Hart-Miller Island is a state park located on the Chesapeake Bay, approximately 22 km from downtown Baltimore.

All measurements were made in the University of Maryland, Baltimore County (UMBC) trailer located on the southeastern side of the island (39.2421° , -76.3627°). Continuous measurements were conducted from 4 June to 5 July 2018. Several gaps in data collection occurred due to periodic power outages on the island.

Comparisons of the HMI measurements were made to two nearby inland sites: Beltsville and Howard University Beltsville (HUB, denoted HU-Beltsville hereafter), approximately 46 and 50 km southwest of HMI, respectively. Beltsville (39.0280° , -76.8171°) is a National Atmospheric Deposition Program Ammonia Monitoring Site (AMoN, <http://nadp.slh.wisc.edu/amon/>, last access: 28 July 2021) and was used for gas-phase NH_3 comparisons. HUB (39.0553° , -76.8783°) is a regulatory monitoring site maintained and operated by MDE and was used for comparisons of speciated $\text{PM}_{2.5}$ concentrations.

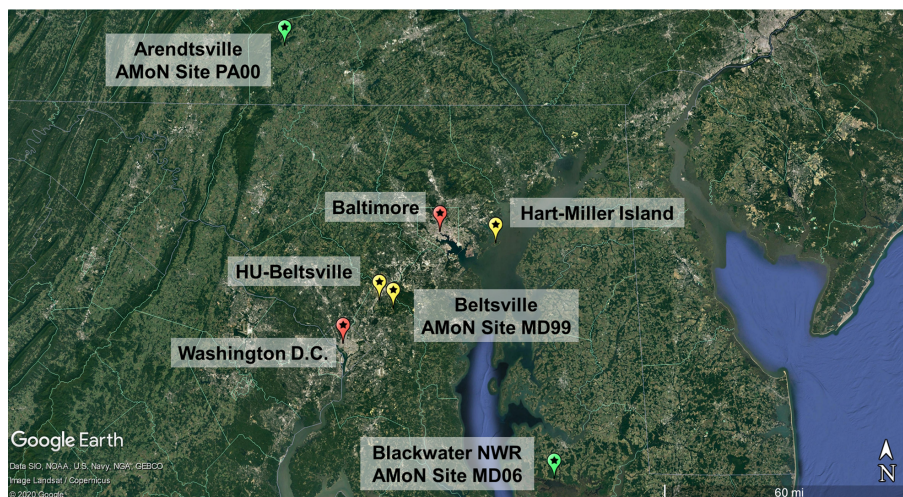


Figure 1. Map of relevant locations for the field campaign. Yellow stars indicate sites used for primary comparison (HMI, Howard University–Beltsville, Beltsville), green stars are locations used for secondary comparisons (Arendtsville, Blackwater), and red stars are labeled for spatial reference (Baltimore, Washington D.C.).

2.2 NH₃ measurements

An AiRRmonia analyzer (RR Mechatronics, the Netherlands) was deployed for measurements of gas-phase ammonia (Norman et al., 2009). The analyzer was enclosed in a weatherproof aluminum box (non-temperature controlled) and placed on top of the UMBC trailer (~ 4 m inlet height). The AiRRmonia uses a 5 cm stainless-steel inlet (i.d. = 0.2 cm) to minimize sampling artifacts associated with gas adsorption to inlet surfaces (Schmohl et al., 2001; Ellis et al., 2010; von Bobruzki et al., 2010). The instrument samples air at a rate of 1 L min⁻¹, giving a gas residence time of ~ 0.01 s in the inlet. Ammonia in the sampled air is absorbed through a gas-permeable polytetrafluoroethylene membrane into an acidic aqueous stripping solution with close to 100 % collection efficiency (Wyers et al., 1993). NaOH is then added to raise the pH so that the collected NH₃ (present as NH₄⁺) is shifted to the NH₃ form, facilitating transfer of NH₃ through another gas-permeable membrane into a separate flow of deionized water. Dual conductivity detectors measure the difference in conductivity between the deionized water before and after this transfer, enabling quantification of sampled NH₃ (Norman et al., 2009; von Bobruzki et al., 2010). The temperature-dependent conductivity was calibrated approximately daily during OWLETS-2 using aqueous NH₄⁺ standards. The instrument's operating principles, including gas collection efficiency and lack of response to aerosol NH₄⁺, have been characterized previously (Wyers et al., 1993; Erisman et al., 2001). The NH₃ measurements during OWLETS-2 were conducted with 10 min resolution.

2.3 PILS-IC

Speciated inorganic PM_{2.5} measurements were made with a particle-into-liquid sampler (PILS) coupled to dual anion-cation ion chromatographs (IC, model 850 Dual IC, Metrohm), collectively referred to as the PILS-IC (Orsini et al., 2003). Ambient air was sampled at 16.0 L min⁻¹ through a PM_{2.5} cyclone (URG Corp.) and two annular denuders in series (URG Corp.) to remove acidic (e.g., HNO₃, HCl) and basic gases (e.g., NH₃). The PILS sample was split and simultaneously analyzed for concentrations of both cations (Na⁺, NH₄⁺, K⁺, Ca²⁺, and Mg²⁺) and anions (Cl⁻, NO₃⁻, SO₄²⁻, and C₂O₄²⁻) according to Valerino et al. (2017).

For anion analysis, the IC utilized a Metrosep A Supp 5 column (150 mm × 4.0 mm) with 1.0 mM NaHCO₃ and 3.2 mM Na₂CO₃ eluent at a flow rate of 0.7 mL min⁻¹. For cation analysis, the IC utilized a Metrosep C 4 column (150 mm × 4.0 mm) that was run with 2.5 mM HNO₃ and 0.5 mM C₂H₂O₄ eluent at a flow rate of 0.9 mL min⁻¹. In the anion analysis, conductivity measurements were preceded by chemical suppression to reduce conductivity of the eluent. This configuration of the PILS-IC resulted in a limit of detection of 0.01 µg m⁻³ (air concentration) for each ion and a 5 min integrated sample every 20 min.

2.4 HYSPLIT model

The HYbrid Single-Particle Lagrangian Integrated Trajectory (HYSPLIT, <https://www.ready.noaa.gov/HYSPLIT.php>, last access: 28 July 2021) model was utilized to investigate source influences during OWLETS-2 (Stein et al., 2015). The model allows for air parcel trajectories, including the back-trajectory analyses used here, to infer regional source influences for the air masses sampled at HMI. High-Resolution

Rapid Refresh (HRRR) 3 km meteorological data were used in generating back-trajectories. The uncertainty and limitations of the HYSPLIT model are worth noting here, especially in accounting for small-scale circulations. As a result, for all events discussed below, HYSPLIT trajectories were crosschecked with measured surface wind conditions and vertical wind fields measured from the meteorological station and a Doppler wind lidar (Leosphere Windcube 200S) deployed at HMI. Meteorological measurements of temperature, relative humidity, and surface wind speed and direction were made with the Vaisala MAWS201 meteorological station at 1 min resolution throughout the study.

3 Results and discussion

3.1 Ammonia

During the OWLETS-2 campaign, gas-phase ammonia was characterized by unusually high concentrations. The average NH_3 concentration ($3.83 \mu\text{g m}^{-3}$) at HMI was more than 3 times greater than NH_3 at the Beltsville AMoN site ($1.20 \mu\text{g m}^{-3}$) during the summer of 2018 (Fig. 2a), a difference that was statistically significant at the 99 % confidence level (p value < 0.01). While average summertime NH_3 shows an increasing trend at Beltsville, the concentrations measured at HMI in 2018 far exceed recent summertime levels at Beltsville. The HMI NH_3 concentrations were also compared to two other AMoN sites (Fig. 1): Blackwater (~ 90 km from HMI; 38.4449° , -76.1112°) and Arendtsville (~ 110 km from HMI; 39.9231° , -77.3078°). Both of these sites are located in much closer proximity to strong agricultural NH_3 emissions, as Blackwater is located on the Eastern Shore of Maryland and Arendtsville is located in southeastern Pennsylvania. Their average summer NH_3 concentrations for 2018 were 57 % (Blackwater, $1.66 \mu\text{g m}^{-3}$) and 49 % (Arendtsville, $1.96 \mu\text{g m}^{-3}$) lower than those measured at HMI during OWLETS-2. In a previous deployment of the AiRRmonia analyzer at the Beltsville AMoN site (unpublished work), the average concentrations measured by the AiRRmonia over a 2-week span (6–20 September 2016) were within $\sim 0.5 \mu\text{g m}^{-3}$ of the colocated AMoN NH_3 measurements, suggesting that systematic measurement differences are not responsible for the trends seen in Fig. 2a.

3.2 Impact on aerosol composition

Before investigating the sources of such high NH_3 concentrations, we first characterize the effects on aerosol composition, because NH_3 contributes significantly to secondary aerosol formation (Seinfeld and Pandis, 2016). Note that our companion paper analyzes the effects of the high NH_3 concentrations on aerosol liquid water and acidity (pH) (Battaglia Jr. et al., 2021).

In the US, SO_4^{2-} concentrations have decreased due to regulations and economic factors that have reduced SO_2 emis-

sions (Hand et al., 2012a). This trend is evident at HU-Beltsville (Fig. 2b), where the average summertime SO_4^{2-} concentration has decreased by more than a factor of 8 since 2007 ($8.23 \mu\text{g m}^{-3}$ versus $0.94 \mu\text{g m}^{-3}$). Note that the data shown in Fig. 2 only include the summer months (June, July, and August) to facilitate direct comparisons to the conditions during OWLETS-2. In contrast to the NH_3 results, the average SO_4^{2-} concentration at HMI ($1.11 \mu\text{g m}^{-3}$) was quite close to the average concentration at HUB ($0.94 \mu\text{g m}^{-3}$), a difference that was not significant at the 95 % confidence level (p value > 0.1). This suggests that the high NH_3 concentrations at HMI did not have a large effect on particulate sulfate mass concentrations, consistent with the understanding of SO_4^{2-} thermodynamics and results from a study in the southeast US (Weber et al., 2016). The agreement in SO_4^{2-} concentrations between HMI and HU-Beltsville is unsurprising given the regional nature of SO_2 emissions and the low spatial variability of SO_4^{2-} levels in the eastern US (Beyersdorf et al., 2016).

While SO_4^{2-} concentrations were typical for the region, the elevated NH_3 did affect the particulate NH_4^+ and NO_3^- concentrations. An ammonia-rich environment, defined when $[\text{Total Ammonia}] > 2 \times [\text{Total Sulfate}]$, can facilitate NH_4NO_3 aerosol formation (Seinfeld and Pandis, 2016). The system measured at HMI was ammonia rich for approximately 25 % of the OWLETS-2 campaign.

As shown in Fig. 2c, the average NH_4^+ concentration at HMI was more than 50 % higher than the summertime average at HU-Beltsville ($0.38 \mu\text{g m}^{-3}$ and $0.23 \mu\text{g m}^{-3}$, respectively), which is statistically significant at the 99 % confidence level (p value < 0.01). The NH_4^+ concentrations at HMI were higher than any of the past five summertime averages measured at HU-Beltsville, demonstrating the influence of elevated NH_3 . Aerosol NO_3^- was also significantly elevated at HMI compared to historical and 2018 summertime levels at HU-Beltsville (Fig. 2d). The HMI average NO_3^- ($0.36 \mu\text{g m}^{-3}$) was more than a factor of 2 higher than at HU-Beltsville ($0.14 \mu\text{g m}^{-3}$), which is also significant at the 99 % confidence level (p value < 0.01). The NO_3^- concentrations at HMI were also higher than typical summertime levels in the eastern US (Sickles II and Shadwick, 2008). The high average NO_3^- concentration during OWLETS-2 was heavily influenced by several peak events where the NO_3^- concentration exceeded $3 \mu\text{g m}^{-3}$ (Fig. S1).

Another notable aspect of the NO_3^- observed during OWLETS-2 was the diurnal profile (Fig. S2a). Formation of NH_4NO_3 is favored by both lower temperature and higher relative humidity (Stelson and Seinfeld, 1982). Thus, the observed midday peak in NO_3^- coincided with the most unfavorable meteorological conditions (Fig. 1 in Battaglia Jr. et al., 2021). More typical summertime diurnal profiles of NO_3^- in the eastern US exhibit a maximum around 06:00–07:00 LT and an afternoon minimum (Xu et al., 2015; Poulain et al., 2011; Weber, 2003; Wittig et al., 2004). The

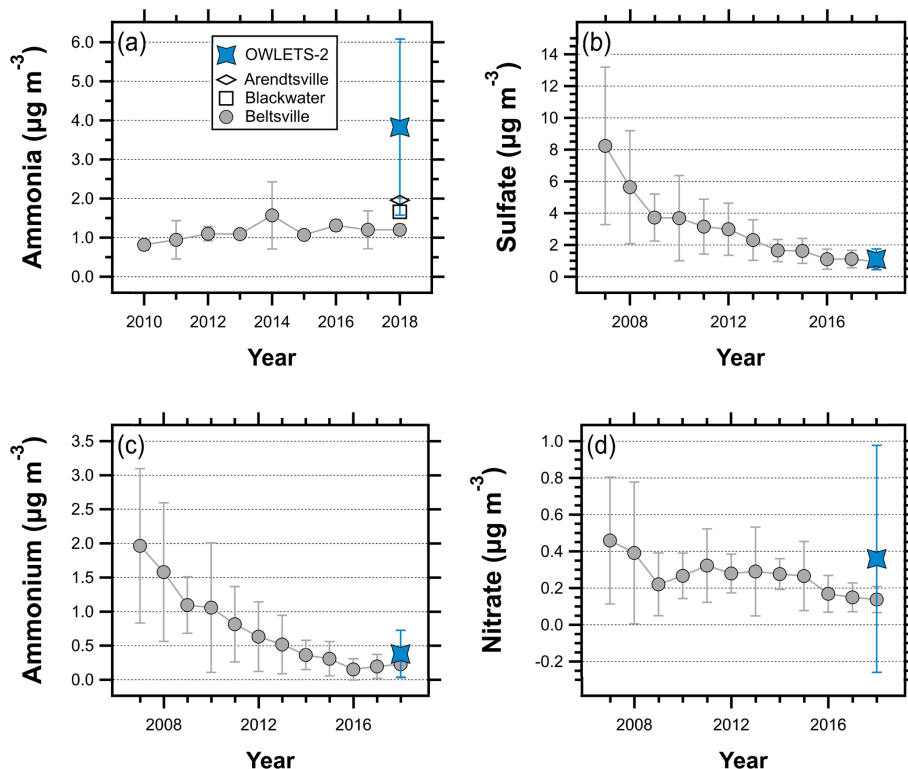


Figure 2. Summertime (June, July, and August) comparisons of (a) NH_3 concentrations measured at HMI, Beltsville, Arendtsville, and Blackwater; (b) $\text{PM}_{2.5}$ SO_4^{2-} measured at HMI and HUB; (c) $\text{PM}_{2.5}$ NH_4^+ measured at HMI and HUB; and (d) $\text{PM}_{2.5}$ NO_3^- measured at HMI and HUB. Error bars represent plus or minus the standard deviation.

NO_3^- diurnal profile observed during OWLETS-2 indicates the important effect of the elevated NH_3 during the campaign and will be discussed in more detail below.

NH_4^+ and NO_3^- concentrations were elevated at HMI compared to the historical data (Fig. 2). In the eastern US, the $\text{PM}_{2.5}$ mass fraction of NH_4NO_3 peaks in the winter with a minimum in the summer (Wittig et al., 2004). Ammonium sulfate, however, is consistently one of the largest fractions of $\text{PM}_{2.5}$ mass in the eastern US (Hand et al., 2012b). For the OWLETS-2 study, the coefficient of determination (R^2) for the linear correlation (least squares regression analysis) between $2 \times (\text{SO}_4^{2-} + \text{NO}_3^-)$ and NH_4^+ was 0.90 (Fig. 3), while the R^2 value for the linear relationship between SO_4^{2-} and NH_4^+ was only 0.57 (not shown), indicating the importance of NH_4NO_3 and the ammonia-rich conditions during OWLETS-2.

Finally, it should be noted that NO_3^- concentrations can be affected by interactions between nitric acid and sodium chloride (Seinfeld and Pandis, 2016). This can have a large impact on aerosol composition in coastal urban areas (Athanasopoulou et al., 2008). However, sodium chloride aerosols, while observed periodically in the fine mode during the campaign, were not frequent enough or high enough in magnitude (max $\text{Na} + \text{Cl} = 0.91 \mu\text{g m}^{-3}$) to suggest a strong influence of primary aerosol emissions from the Chesapeake Bay.

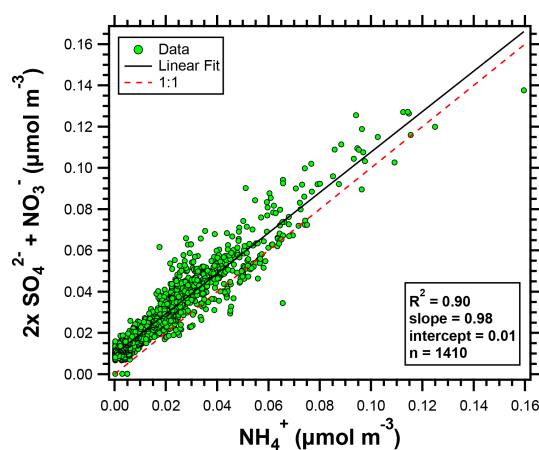


Figure 3. Scatter plot of $2 \times (\text{SO}_4^{2-} + \text{NO}_3^-)$ versus NH_4^+ (all species in molar concentrations) for the OWLETS-2 campaign.

3.3 Characterization of ammonia sources

Source locations of the high NH_3 events were investigated using the NOAA HYSPLIT model. Trajectories produced by the model were checked for consistency with vertical wind fields measured by Doppler wind lidar (when available, with the one discrepancy noted in Table 1). Back-

trajectories were initialized from HMI (50 m altitude) at the time corresponding to each NH_3 measurement. Air mass back-trajectories were run based upon a recent study's estimate of 15 h for the average NH_3 lifetime (Hauglustaine et al., 2014), though other studies have estimated much lower NH_3 lifetimes for point sources (Dammers et al., 2019). Figure 4 shows the ensemble of all back-trajectories for the campaign colored by the measured NH_3 concentration. Overall, the back-trajectory origins were consistent with predominant surface winds during the campaign. Figure 4 also shows that elevated NH_3 concentrations were not limited to trajectories originating from a single direction or region.

A subset of the trajectories in Fig. 4 was further investigated to identify the potential sources of peak NH_3 events. When both particle-phase and gas-phase ammonia were measured, total ammonia and gas-phase ammonia correlated strongly ($R = 0.9927$), showing that gas-phase ammonia is an effective tracer for total ammonia for this campaign. Eleven distinct events had peak NH_3 concentrations above the 95th percentile ($> 7.96 \mu\text{g m}^{-3}$) for the OWLETS-2 study (Fig. 5). Back-trajectories for each event are shown in Fig. 6. Altitudes of all back-trajectories were below 1 km over the postulated source region.

Agriculture represents the largest source of atmospheric NH_3 emissions globally (Sutton et al., 2013). Agricultural NH_3 emissions stem from fertilizer and livestock management (Pinder et al., 2006). Previous studies have linked high livestock NH_3 emissions with particulate nitrate formation (Xu et al., 2019; Paulot et al., 2016; Sorooshian et al., 2008). HMI is located in relatively close proximity to several areas of concentrated livestock production (Fig. 7). To the east and southeast of HMI, the Delmarva Peninsula (Delaware–Maryland–Virginia) is a large poultry producing region. The emissions from these chicken houses have been characterized by ground measurements (Siefert et al., 2004) and captured by satellite measurements (Warner et al., 2017). Additionally, there are large concentrations of dairy cows in southeastern Pennsylvania, also shown in Fig. 7. The NH_3 emissions in this area are some of the highest in the country for dairy cows (Pinder et al., 2004b). While dairy cow populations are relatively minor in Maryland, poultry emissions could be a significant emitter in the same region of Pennsylvania where dairy cows are concentrated (Fig. S3). The back-trajectories identify events 1, 2, 4, 5, 6, 7, and 11 as having likely agricultural influence (Table 1), consistent with the agricultural hotspots identified here (Figs. 7, S3). Additionally, the source for event no. 3 is ambiguous, but has the potential to be the poultry sources discussed above.

While agricultural emissions were the likely source of many peak events, several events – including the highest NH_3 concentration measured during the campaign – appear to have a nonagricultural origin. Specifically, the trajectories for event nos. 8–10 pass directly over the city of Baltimore and do not appear to intersect with any major agricultural sources in the 15 h prior to arrival at HMI. A number of ur-

ban and industrial NH_3 sources are known, including motor vehicles (Bishop and Stedman, 2015; Sun et al., 2017) and fertilizer production plants (Van Damme et al., 2018). Ammonia is produced when proteins are broken down under anaerobic conditions (Rittmann and McCarty, 2001), causing landfills (Sutton et al., 2000), waste composting and processing (Sutton et al., 2013; Pagans et al., 2006), and wastewater treatment plants (Reche et al., 2015; Artíñano et al., 2018) to emit significant quantities of NH_3 , as well.

The contribution of traffic to event nos. 8–10 was likely quite small due to a combined R^2 value of 0.201 between NH_3 and CO for the duration of the three events (based on CO measurements colocated at HMI). NH_3 and CO are correlated in vehicle emissions (Kean et al., 2009; Perrino et al., 2002); however, for these events, high NH_3 was observed without a spike in CO. We acknowledge that order-of-magnitude differences in the atmospheric lifetimes of CO and NH_3 would alter correlations downwind from sources co-emitting both pollutants, but in this case, the species with the longer lifetime (CO) did not show an enhancement during the NH_3 events, suggesting mobile sources were not a significant factor here. The trajectories for event nos. 8–10 identify a cluster of potential industrial NH_3 sources (Fig. 8).

The potential NH_3 sources for event nos. 8–10 include the Back River Wastewater Treatment Plant (A in Fig. 8), the Patapsco Wastewater Treatment Plant (B), a W.R. Grace Chemical Production Facility (C), the Quarantine Road Landfill (D), a large-scale composting facility (E), and Yara Fertilizer Distributor (F). Of these facilities, only W.R. Grace (224.1 tyr^{-1}) and the composting facility (1.03 tyr^{-1}) are permitted to release NH_3 by the state of Maryland (MDE, 2019a, b). However, the non-permitted sites are likely major NH_3 emitters, based upon urban NH_3 sources previously identified in the literature. It is likely that emissions from multiple sources collectively contributed to NH_3 levels during these events; however, the potential sources are too close together to distinguish or estimate individual contributions.

It is important to note that numerous back-trajectories also passed over this cluster of industrial sources during times when NH_3 was not elevated. However, event nos. 8–10 share characteristics that explain the high NH_3 levels at HMI. The peak concentration of each event occurred between 07:00–08:00 LT (Table 1). Additionally, the events had extremely low wind speeds of 0.8, 0.7, and 0.6 ms^{-1} , respectively, all well below the campaign average of 2.9 ms^{-1} (Table 1). These values were below the 10th percentile of all wind speeds measured at HMI during OWLETS-2.

With such low wind speeds, transport time for the $\sim 18 \text{ km}$ distance between the cluster of NH_3 sources near downtown Baltimore and HMI would be $\sim 7\text{--}8 \text{ h}$ for event nos. 8–10, suggesting that the original emissions occurred near midnight. Low wind speeds occurring at night correspond to the most stable atmospheric conditions and to a low boundary layer, which together enable elevated pollutant concentrations downwind of point sources (Arya, 1999).

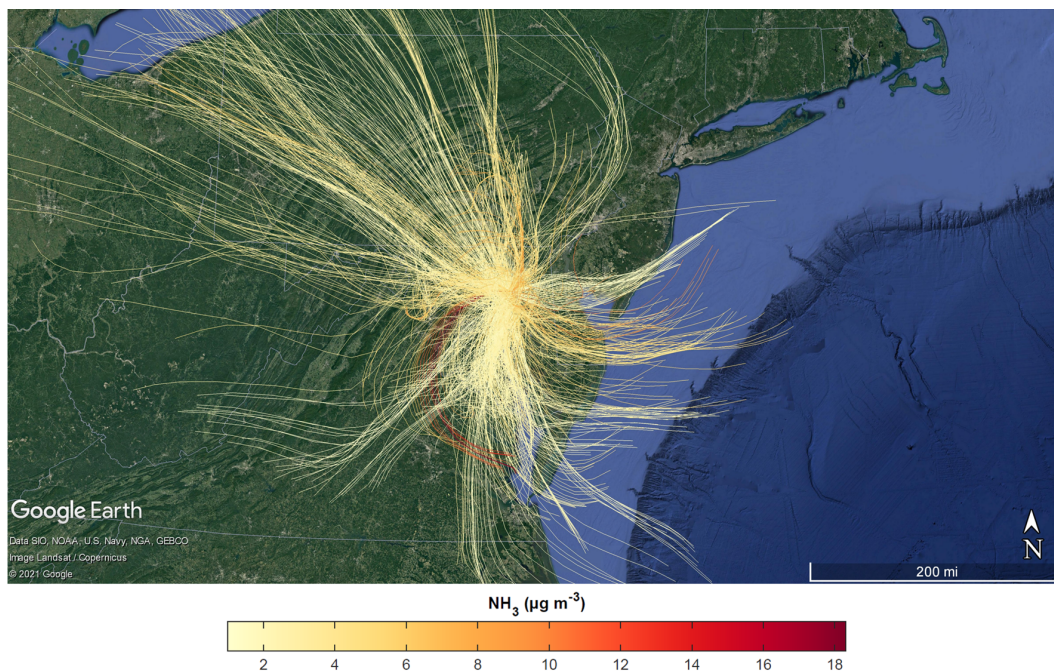


Figure 4. Aggregate 15 h HYSPLIT back-trajectories initialized at HMI (50 m altitude) and colored by NH_3 concentrations measured at HMI utilizing 3 km HRRR meteorology. Every other back-trajectory is displayed for clarity.

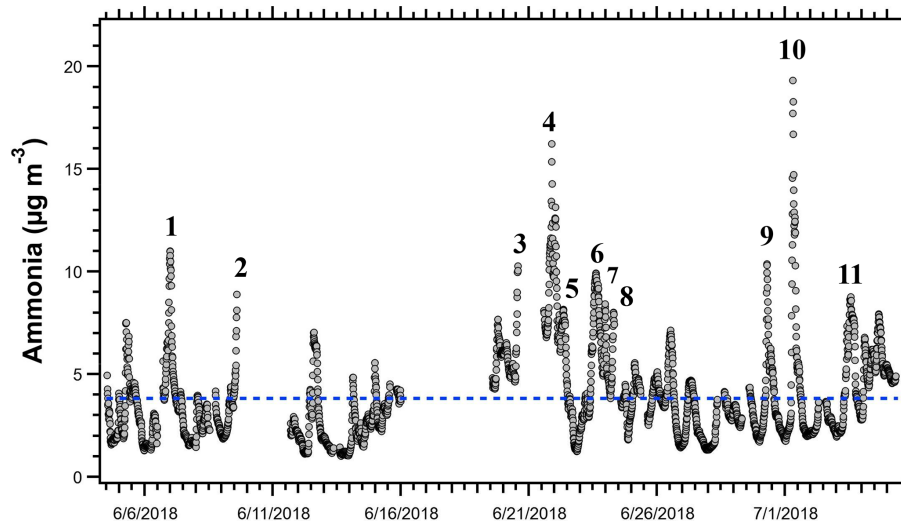


Figure 5. Time series of NH_3 measurements at HMI during OWLETS-2. The 11 NH_3 peak events are labeled and represent the concentrations above the 95th percentile for the entire data set ($7.96 \mu\text{g m}^{-3}$). Gaps in data are due to power outages that occurred on the island. Events 2 and 3 were cut off by power outages. The blue dashed line represents the campaign-average NH_3 concentration ($3.83 \mu\text{g m}^{-3}$).

For example, event no. 10 had a peak NH_3 concentration $\sim 15.5 \mu\text{g m}^{-3}$ higher than the campaign average ($3.8 \mu\text{g m}^{-3}$). Under Pasquill–Gifford stability class F (nighttime, low winds), the required point source emission rate is 2 orders of magnitude lower (1 g s^{-1} vs. 172 g s^{-1}) than it is under stability class B (slight daytime solar radiation, low winds) to give the same $15.5 \mu\text{g m}^{-3}$ NH_3 enhancement at HMI. This illustrative example shows the potential for atmospheric stabil-

ity to impact downwind surface concentration enhancement. Specifically, for this study, urban sources with moderate NH_3 emissions can have a profound effect on downwind NH_3 levels under the most stable atmospheric conditions.

Further, event nos. 8–10 also occurred shortly before onsets of the Chesapeake Bay breeze. The convergence between an offshore synoptic flow and the breeze creates a period of stagnation or calm winds that favor the accumulation of pol-

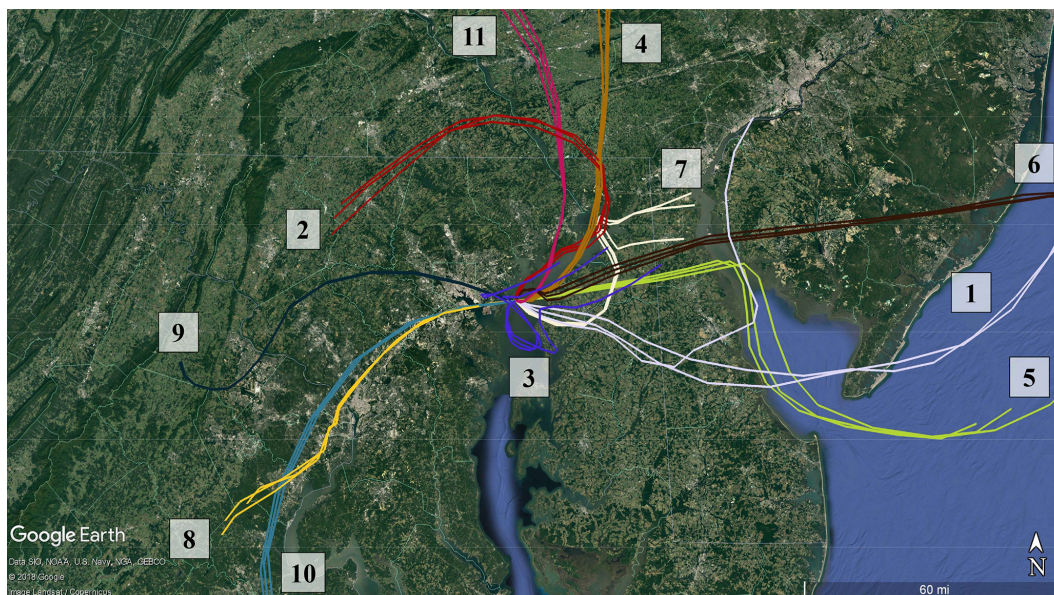


Figure 6. HYSPLIT back-trajectories initialized at HMI using 3 km HRRR meteorology and an altitude of 50 m for the peak NH_3 events identified in Fig. 5. There are three trajectories for each event: one for the highest concentration of the event, one 10 min earlier, and one 10 min later.

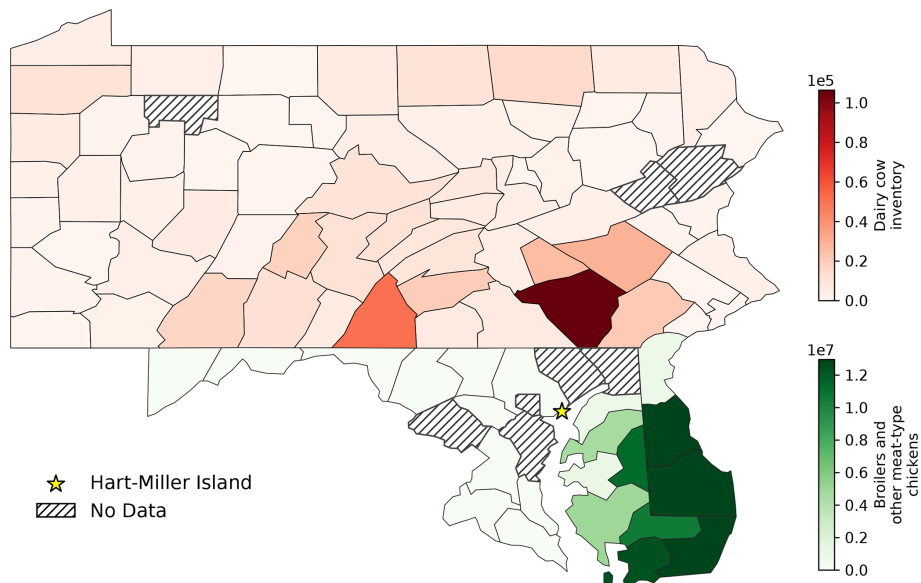


Figure 7. Inventories of dairy cows in Pennsylvania and broiler and other meat-type chickens in Maryland and Delaware. Data are from the 2017 Census of Agriculture (USDA, 2017).

lutants (Caicedo et al., 2019; Loughner et al., 2014). Additionally, the early morning occurrence of event nos. 8–10 also suggests that a low dilution volume as the marine boundary layer is only beginning its convective regime (Stull, 1988). Combined, calm winds and relatively shallow boundary layers are important factors contributing to the high NH_3 concentrations.

Natural sources of NH_3 can represent the dominant source of emissions in some regions (Paulot et al., 2015; Sutton et al., 2013). The Chesapeake Bay can be a source or sink for NH_3 in the summertime (Larsen et al., 2001); however, the emission factors reported by Larsen et al. (2001) suggest a relatively minor influence of Chesapeake Bay emissions compared to the agricultural and industrial sources discussed above.

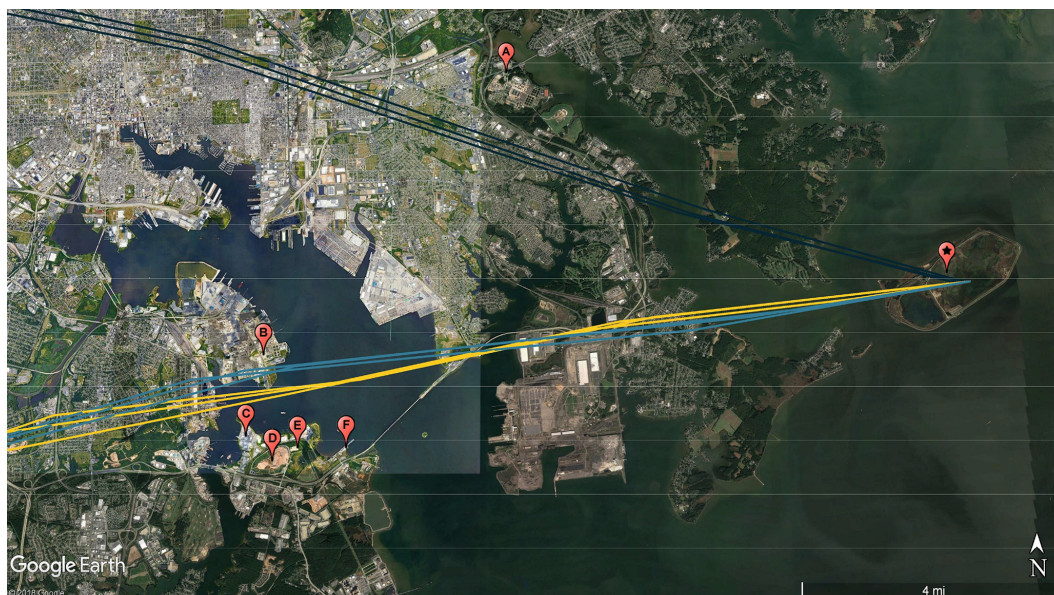


Figure 8. Back-trajectories initialized at HMI (star) using 3 km HRRR meteorology for event nos. 8 (yellow), 9 (dark blue), and 10 (teal). Potential industrial sources of NH_3 are (A) Back River Wastewater Treatment Plant, (B) Patapsco Wastewater Treatment Plant, (C) W.R. Grace Facility, (D) Quarantine Road Landfill, (E) a composting facility, and (F) Yara Fertilizer Distributor.

Table 1. Description of peak NH_3 events.

Event no.	Peak NH_3 ($\mu\text{g m}^{-3}$)	Time (local time)	Temperature ($^{\circ}\text{C}$)	Wind speed previous 8 h average (m s^{-1})	Source
1	11.0	6 June 2018 23:40	18.9	2.68	Poultry
2	8.89	9 June 2018 14:45	24.6	2.09	Dairy
3	10.3	20 June 2018 13:44	27.7	2.33	Ambiguous
4	16.2	21 June 2018 19:29	25.3	2.16	Dairy
5	8.16	22 June 2018 08:19	22.5	4.50	Poultry
6	9.93	23 June 2018 14:49	22.7	3.18	Poultry
7	8.42	23 June 2018 23:39	23.9	2.08	Poultry
8	8.02	24 June 2018 07:19	24.5	0.79	Industrial
9	10.4	30 June 2018 07:15	26.3	0.67	Industrial
10	19.3	1 July 2018 07:35	27.8	0.61	Industrial
11	8.77	3 July 2018 13:42	31.7	1.77	Dairy

Events 2 and 3 were cut short by power outages. Event 2 (one of the two events where wind lidar data were not available for crosschecking the back-trajectory) is the only event with a discrepancy between HYSPLIT (predicts wind direction coming from NNE) and observations (measured surface wind direction coming from E).

3.4 Temperature effects

Temperature plays an important role in NH_3 emissions from fertilizer and animal waste (Robarge et al., 2002; Pleim et al., 2013). This contributes to strong seasonal and diurnal profiles of agricultural NH_3 emissions (Warner et al., 2017; Zhu et al., 2015; Pinder et al., 2004a). The average diurnal profile of NH_3 (Fig. 9a) shows enhanced concentrations between the hours of 07:00–15:00 LT, consistent with temperature-driven emissions. Overall, NH_3 concentrations rose with increasing temperature (Fig. 9b); however, there was a lot of scatter in the data ($R^2 = 0.05$ for individual (10 min) measurements of

NH_3 –temperature over the entire campaign). In the absence of strong local sources of NH_3 emissions, ambient observations are most impacted by transport. At HMI, this includes diverse source sectors from different areas that correspond to various time lags in emission to observation. This confounds strict interpretation of temperature-dependent emission relationships.

3.5 Deposition effects

Several factors likely explain why the NH_3 concentrations observed at HMI were more than 3 times higher than those

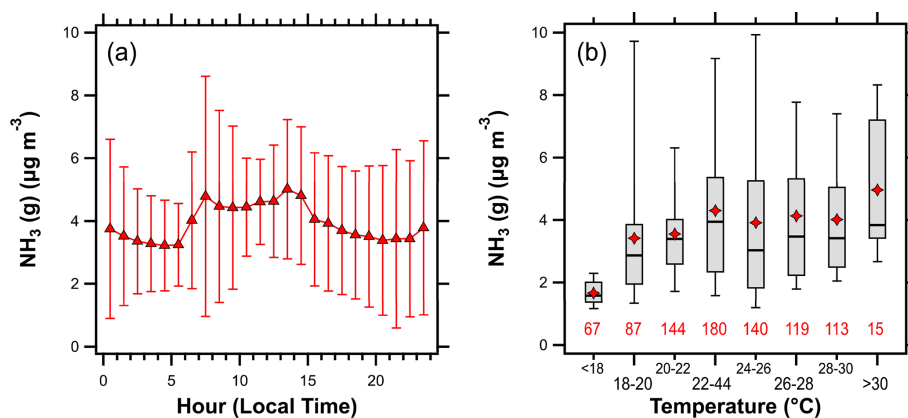


Figure 9. (a) The diurnal profile of NH_3 (error bars represent plus or minus the standard deviation) and (b) box plot showing variations in the NH_3 concentration with temperature. Lines in (b) represent the 5th, 25th, 50th, 75th, and 95th percentiles; diamonds represent the mean, while numbers beneath each box represent the number of observations in each temperature interval.

observed at Beltsville (Fig. 2a). Due to differences in proximity to the city of Baltimore (Beltsville is ~ 45 km from downtown Baltimore) and to the Chesapeake Bay (e.g., bay breeze circulation), Beltsville was not affected by the identified industrial areas as severely as Hart-Miller Island. Further, when the wind direction may have facilitated transport from downtown Baltimore to Beltsville, the atmospheric conditions were not typically stable, giving rise to much lower downwind concentrations. However, the trajectory analysis (not shown) indicates that Beltsville frequently received air masses that had recently passed over the agricultural areas of the Delmarva Peninsula, the most common source of extreme NH_3 concentrations at HMI (Table 1).

The most likely explanation for the higher concentrations at HMI is a dramatic difference in the bidirectional flux of NH_3 during transport to each site. The path from the Delmarva Peninsula to Hart-Miller Island consists primarily of transport over water (the Chesapeake Bay), while the path for transport to Beltsville includes significantly more time and distance over land (~ 40 km). The dry deposition velocity of gases is typically lower over water than over land, especially forested regions like the land surrounding the Beltsville AMoN site (Li et al., 2019). Additionally, the Chesapeake Bay can be a net source of NH_3 during the summer (Larsen et al., 2001), suggesting deposition can be, on a net basis, quite small over the body of water. A recent modeling study found that reactive nitrogen undergoes much higher rates of dry deposition to the coastline bordering the Chesapeake Bay compared to rates over water (Loughner et al., 2016). The NH_3 measurements at Beltsville are 2-week integrated samples, precluding a direct comparison to the HMI measurements and quantitative estimates of NH_3 lost to dry deposition during transport. However, dry deposition of NH_3 is a key uncertainty in accurate NH_3 predictions (Pleim et al., 2013), so future studies should examine this question directly. The dry deposition of NH_3 and HNO_3 are affected by

the aerosol liquid water content and particle pH (Nenes et al., 2021), and this will be analyzed in our companion paper.

4 Conclusions

Semicontinuous measurements of aerosol chemical composition and gas-phase NH_3 were carried out during summer 2018 as part of the OWLETS-2 field campaign. The measurement site was located in close proximity to the land–water transition between the Chesapeake Bay and downtown Baltimore, MD. Sulfate levels were in line with historical trends and with concentrations measured at the same time in other locations near Baltimore. However, average aerosol NO_3^- and NH_4^+ concentrations were significantly elevated compared to the average concentrations at a regulatory monitoring site ~ 45 km away. The elevated aerosol concentrations were likely driven by gas-phase NH_3 , as higher background levels and episodic spikes contributed to average NH_3 concentrations that were more than 3 times higher than the average levels measured at a nearby (~ 45 km) AMoN site.

An array of sources likely contributed to the elevated NH_3 concentrations. Agricultural emissions from poultry operations in the Delmarva Peninsula and dairy cattle in southeastern Pennsylvania were the most frequent sources of high NH_3 at HMI. Low dry deposition velocities over the Chesapeake Bay enabled efficient transport of NH_3 (and likely HNO_3 , as well) to the site. Under stable atmospheric conditions, industrial NH_3 emissions from a cluster of sources near downtown Baltimore also contributed to several peak NH_3 events, including the highest NH_3 concentrations measured during OWLETS-2 ($> 19 \mu\text{g m}^{-3}$). These observations demonstrate the complex interplay between emissions, transport, and meteorology in affecting urban aerosol chemistry. Our companion study examines the effects of the unique meteorology and high NH_3 concentrations on aerosol liquid water content and acidity (pH) (Battaglia Jr. et al., 2021).

Prior studies have shown that sulfate is regional in nature in the eastern US, exhibiting low spatial variability over tens of kilometers (Beyersdorf et al., 2016). Our results are consistent with these findings, suggesting that meteorological phenomena such as the bay breeze circulation or urban heat islands (Battaglia et al., 2017) do not substantially alter sulfate levels in this region. On the contrary, our results suggest strong gradients of reactive nitrogen species in the aerosol and gas phases, which will also produce periodic spatial gradients (including episodic spikes) in PM_{2.5} mass. The relatively short duration of these events and their dependence on proximity to water suggests they may not be well captured by regulatory monitoring (or longer-term monitoring for deposition networks). These results likely have implications for atmospheric chemistry and air quality in other coastal cities, including those outside of the eastern US. Our results suggest that analyses of urban air quality may be more illuminating if the urban areas are, themselves, segregated into coastal and inland locations. For example, the AeroCom study evaluated a number of global aerosol models using predictions in urban and remote locations as key indicators of model predictive skill (Tsigaridis et al., 2014). Our results highlight important differences in sources and processes affecting coastal versus inland urban areas that may have a determining effect on aerosol composition and concentrations.

Code availability. Publicly available code (<https://github.com/AirChem/HYSPLITcontrol>, Wolfe, 2021) was used to run back-trajectories in bulk and scale their color by user-input data (code courtesy of Glenn Wolfe, NASA/GSFC and UMBC/JCET).

Data availability. Data are available at <https://www-air.larc.nasa.gov/cgi-bin/ArcView/owllets.2018> (NASA, 2021).

Supplement. The supplement related to this article is available online at: <https://doi.org/10.5194/acp-21-13051-2021-supplement>.

Author contributions. CJH, AGC, and RD conceived the analysis and study participation. MAB Jr., NB, and KB collected and analyzed the PILS-IC and NH₃ data. NB and CJH conducted the trajectory and source identification analyses. VC and AGC provided analytical input and interpretation. NB and CJH wrote the article. All authors provided feedback and revisions to the article.

Competing interests. The contact author has declared that neither they nor their co-authors have any competing interests.

Disclaimer. Publisher's note: Copernicus Publications remains neutral with regard to jurisdictional claims in published maps and institutional affiliations.

Acknowledgements. Annmarie G. Carlton and Christopher J. Hennigan acknowledge funding from the National Science Foundation, AGS-1719252 and AGS-1719245. Ruben Delgado and Vanessa Caicedo acknowledge support by the Maryland Department of the Environment (contract no. U00P8400651). Nicholas Balasus and Katherine Ball received support through the NOAA Office of Education, Educational Partnership Program with Minority Serving Institutions (EPP/MSI) and the Cooperative Science Center for Earth System Sciences and Remote Sensing Technologies (grant no. NA16SEC4810008).

Financial support. This research has been supported by the National Science Foundation (grant nos. AGS-1719252 and AGS-1719245), Maryland Department of the Environment (contract no. U00P8400651), and the National Oceanic and Atmospheric Administration (grant no. NA16SEC4810008).

Review statement. This paper was edited by James Allan and reviewed by two anonymous referees.

References

- Adams, P. J., Seinfeld, J. H., and Koch, D. M.: Global concentrations of tropospheric sulfate, nitrate, and ammonium aerosol simulated in a general circulation model, *J. Geophys. Res.-Atmos.*, 104, 13791–13823, <https://doi.org/10.1029/1999JD900083>, 1999.
- Ansari, A. S. and Pandis, S. N.: Response of inorganic PM to precursor concentrations, *Environ. Sci. Technol.*, 32, 2706–2714, <https://doi.org/10.1021/es971130j>, 1998.
- Artiñano, B., Pujadas, M., Alonso-Blanco, E., Becerril-Valle, M., Coz, E., Gómez-Moreno, F. J., Salvador, P., Nuñez, L., Palacios, M., and Diaz, E.: Real-time monitoring of atmospheric ammonia during a pollution episode in Madrid (Spain), *Atmos. Environ.*, 189, 80–88, <https://doi.org/10.1016/j.atmosenv.2018.06.037>, 2018.
- Arya, S. P.: *Air pollution meteorology and dispersion*, vol. 6, Oxford University Press, New York, 1999.
- Athanasopoulou, E., Tombrou, M., Pandis, S. N., and Russell, A. G.: The role of sea-salt emissions and heterogeneous chemistry in the air quality of polluted coastal areas, *Atmos. Chem. Phys.*, 8, 5755–5769, <https://doi.org/10.5194/acp-8-5755-2008>, 2008.
- Backes, A. M., Aulinger, A., Bieser, J., Matthias, V., and Quante, M.: Ammonia emissions in Europe, part II: How ammonia emission abatement strategies affect secondary aerosols, *Atmos. Environ.*, 126, 153–161, <https://doi.org/10.1016/j.atmosenv.2015.11.039>, 2016.
- Battaglia Jr., M. A., Douglas, S., and Hennigan, C. J.: Effect of the urban heat island on aerosol pH, *Environ. Sci. Technol.*, 51, 13095–13103, <https://doi.org/10.1021/acs.est.7b02786>, 2017.
- Battaglia, M. A., Balasus, N., Ball, K., Caicedo, V., Delgado, R., Carlton, A. G., and Hennigan, C. J.: Urban aerosol chemistry at a land-water transition site during summer – Part 2: Aerosol pH and liquid water content, *Atmos. Chem. Phys. Discuss.* [preprint], <https://doi.org/10.5194/acp-2021-368>, in review, 2021.

- Bergström, A.-K. and Jansson, M.: Atmospheric nitrogen deposition has caused nitrogen enrichment and eutrophication of lakes in the northern hemisphere, *Glob. Change Biol.*, 12, 635–643, <https://doi.org/10.1111/j.1365-2486.2006.01129.x>, 2006.
- Beyersdorf, A. J., Ziemba, L. D., Chen, G., Corr, C. A., Crawford, J. H., Diskin, G. S., Moore, R. H., Thornhill, K. L., Winstead, E. L., and Anderson, B. E.: The impacts of aerosol loading, composition, and water uptake on aerosol extinction variability in the Baltimore–Washington, D.C. region, *Atmos. Chem. Phys.*, 16, 1003–1015, <https://doi.org/10.5194/acp-16-1003-2016>, 2016.
- Bian, H., Chin, M., Hauglustaine, D. A., Schulz, M., Myhre, G., Bauer, S. E., Lund, M. T., Karydis, V. A., Kucsera, T. L., Pan, X., Pozzer, A., Skeie, R. B., Steenrod, S. D., Sudo, K., Tsigaridis, K., Tsimpidi, A. P., and Tsyro, S. G.: Investigation of global particulate nitrate from the AeroCom phase III experiment, *Atmos. Chem. Phys.*, 17, 12911–12940, <https://doi.org/10.5194/acp-17-12911-2017>, 2017.
- Bishop, G. A. and Stedman, D. H.: Reactive nitrogen species emission trends in three light-/medium-duty United States fleets, *Environ. Sci. Technol.*, 49, 11234–11240, <https://doi.org/10.1021/acs.est.5b02392>, 2015.
- Bouwman, A., Lee, D., Asman, W., Dentener, F., Van Der Hoek, K., and Olivier, J.: A global high-resolution emission inventory for ammonia, *Global Biogeochem. Cy.*, 11, 561–587, <https://doi.org/10.1029/97GB02266>, 1997.
- Caicedo, V., Rappenglueck, B., Cuchiara, G., Flynn, J., Ferrare, R., Scarino, A., Berkoff, T., Senff, C., Langford, A., and Lefer, B.: Bay breeze and sea breeze circulation impacts on the planetary boundary layer and air quality from an observed and modeled DISCOVER-AQ Texas case study, *J. Geophys. Res.-Atmos.*, 124, 7359–7378, <https://doi.org/10.1029/2019JD030523>, 2019.
- Dammers, E., McLinden, C. A., Griffin, D., Shephard, M. W., Van Der Graaf, S., Lutsch, E., Schaap, M., Gainairu-Matz, Y., Fioletov, V., Van Damme, M., Whitburn, S., Clarisse, L., Cady-Pereira, K., Clerbaux, C., Coheur, P. F., and Erisman, J. W.: NH₃ emissions from large point sources derived from CrIS and IASI satellite observations, *Atmos. Chem. Phys.*, 19, 12261–12293, <https://doi.org/10.5194/acp-19-12261-2019>, 2019.
- de Gouw, J. A., Middlebrook, A. M., Warneke, C., Goldan, P. D., Kuster, W. C., Roberts, J. M., Fehsenfeld, F. C., Worsnop, D. R., Canagaratna, M. R., Pszenny, A. A. P., Keene, W. C., Marchewka, M., Bertman, S. B., and Bates, T. S.: Budget of organic carbon in a polluted atmosphere: Results from the New England Air Quality Study in 2002, *J. Geophys. Res.-Atmos.*, 110, D16305, <https://doi.org/10.1029/2004JD005623>, 2005.
- Ellis, R. A., Murphy, J. G., Pattey, E., van Haarlem, R., O'Brien, J. M., and Herndon, S. C.: Characterizing a Quantum Cascade Tunable Infrared Laser Differential Absorption Spectrometer (QC-TILDAS) for measurements of atmospheric ammonia, *Atmos. Meas. Tech.*, 3, 397–406, <https://doi.org/10.5194/amt-3-397-2010>, 2010.
- Erisman, J. W., Otjes, R., Hensen, A., Jongejan, P., van den Bulk, P., Khlystov, A., Möls, H., and Slanina, S.: Instrument development and application in studies and monitoring of ambient ammonia, *Atmos. Environ.*, 35, 1913–1922, [https://doi.org/10.1016/S1352-2310\(00\)00544-6](https://doi.org/10.1016/S1352-2310(00)00544-6), 2001.
- Guo, H., Nenes, A., and Weber, R. J.: The underappreciated role of nonvolatile cations in aerosol ammonium-sulfate molar ratios, *Atmos. Chem. Phys.*, 18, 17307–17323, <https://doi.org/10.5194/acp-18-17307-2018>, 2018.
- Hand, J. L., Schichtel, B. A., Malm, W. C., and Pitchford, M. L.: Particulate sulfate ion concentration and SO₂ emission trends in the United States from the early 1990s through 2010, *Atmos. Chem. Phys.*, 12, 10353–10365, <https://doi.org/10.5194/acp-12-10353-2012>, 2012a.
- Hand, J., Schichtel, B., Pitchford, M., Malm, W., and Frank, N.: Seasonal composition of remote and urban fine particulate matter in the United States, *J. Geophys. Res.-Atmos.*, 117, D05209, <https://doi.org/10.1029/2011JD017122>, 2012b.
- Hauglustaine, D. A., Balkanski, Y., and Schulz, M.: A global model simulation of present and future nitrate aerosols and their direct radiative forcing of climate, *Atmos. Chem. Phys.*, 14, 11031–11063, <https://doi.org/10.5194/acp-14-11031-2014>, 2014.
- Kean, A., Littlejohn, D., Ban-Weiss, G., Harley, R., Kirchstetter, T., and Lunden, M.: Trends in on-road vehicle emissions of ammonia, *Atmos. Environ.*, 43, 1565–1570, <https://doi.org/10.1016/j.atmosenv.2008.09.085>, 2009.
- Keene, W. C., Moody, J. L., Galloway, J. N., Prospero, J. M., Cooper, O. R., Eckhardt, S., and Maben, J. R.: Long-term trends in aerosol and precipitation composition over the western North Atlantic Ocean at Bermuda, *Atmos. Chem. Phys.*, 14, 8119–8135, <https://doi.org/10.5194/acp-14-8119-2014>, 2014.
- Larsen, R. K., Steinbacher, J. C., and Baker, J. E.: Ammonia Exchange between the Atmosphere and the Surface Waters at Two Locations in the Chesapeake Bay, *Environ. Sci. Technol.*, 35, 4731–4738, <https://doi.org/10.1021/es0107551>, 2001.
- Li, M., Su, H., Li, G., Ma, N., Pöschl, U., and Cheng, Y.: Relative importance of gas uptake on aerosol and ground surfaces characterized by equivalent uptake coefficients, *Atmos. Chem. Phys.*, 19, 10981–11011, <https://doi.org/10.5194/acp-19-10981-2019>, 2019.
- Loughner, C. P., Allen, D. J., Pickering, K. E., Zhang, D.-L., Shou, Y.-X., and Dickerson, R. R.: Impact of fair-weather cumulus clouds and the Chesapeake Bay breeze on pollutant transport and transformation, *Atmos. Environ.*, 45, 4060–4072, <https://doi.org/10.1016/j.atmosenv.2011.04.003>, 2011.
- Loughner, C. P., Tzortziou, M., Follette-Cook, M., Pickering, K. E., Goldberg, D., Satam, C., Weinheimer, A., Crawford, J. H., Knapp, D. J., Montzka, D. D., Diskin, G. S., and Dickerson, R. R.: Impact of bay-breeze circulations on surface air quality and boundary layer export, *J. Appl. Meteorol. Clim.*, 53, 1697–1713, <https://doi.org/10.1175/JAMC-D-13-0323.1>, 2014.
- Loughner, C. P., Tzortziou, M., Shroder, S., and Pickering, K. E.: Enhanced dry deposition of nitrogen pollution near coastlines: A case study covering the Chesapeake Bay estuary and Atlantic Ocean coastline, *J. Geophys. Res.-Atmos.*, 121, 14221–14238, <https://doi.org/10.1002/2016JD025571>, 2016.
- MDE: Baltimore City Composting Facility, General facility information: Emissions certification report, Maryland Department of the Environment Air and Radiation Management Administration, 2019a.
- MDE: Grace Davison, General facility information: Emissions certification report, Maryland Department of the Environment Air and Radiation Management Administration, 2019b.
- Meng, W., Zhong, Q., Yun, X., Zhu, X., Huang, T., Shen, H., Chen, Y., Chen, H., Zhou, F., Liu, J., Wang, X., Zeng, E. Y., and Tao, S.: Improvement of a Global High-Resolution

- Ammonia Emission Inventory for Combustion and Industrial Sources with New Data from the Residential and Transportation Sectors, *Environ. Sci. Technol.*, 51, 2821–2829, <https://doi.org/10.1021/acs.est.6b03694>, 2017.
- NASA: OWLETS 2018 Data, NASA [data], available at: <https://www-air.larc.nasa.gov/cgi-bin/ArcView/owlets.2018>, last access: 28 July 2021.
- Nenes, A., Pandis, S. N., Kanakidou, M., Russell, A. G., Song, S., Vasilakos, P., and Weber, R. J.: Aerosol acidity and liquid water content regulate the dry deposition of inorganic reactive nitrogen, *Atmos. Chem. Phys.*, 21, 6023–6033, <https://doi.org/10.5194/acp-21-6023-2021>, 2021.
- NOAA: National Coastal Population Report: Population Trends from 1970 to 2020, available at: <https://aambpublicoceanservice.blob.core.windows.net/oceanserviceprod/facts/coastal-population-report.pdf> (last access: 30 April 2021), 2013.
- Norman, M., Spirig, C., Wolff, V., Trebs, I., Flechard, C., Wisthaler, A., Schnitzhofer, R., Hansel, A., and Neftel, A.: Intercomparison of ammonia measurement techniques at an intensively managed grassland site (Oensingen, Switzerland), *Atmos. Chem. Phys.*, 9, 2635–2645, <https://doi.org/10.5194/acp-9-2635-2009>, 2009.
- Orsini, D. A., Ma, Y., Sullivan, A., Sierau, B., Baumann, K., and Weber, R. J.: Refinements to the particle-into-liquid sampler (PILS) for ground and airborne measurements of water soluble aerosol composition, *Atmos. Environ.*, 37, 1243–1259, [https://doi.org/10.1016/S1352-2310\(02\)01015-4](https://doi.org/10.1016/S1352-2310(02)01015-4), 2003.
- Pagans, E., Barrena, R., Font, X., and Sánchez, A.: Ammonia emissions from the composting of different organic wastes. Dependency on process temperature, *Chemosphere*, 62, 1534–1542, <https://doi.org/10.1016/j.chemosphere.2005.06.044>, 2006.
- Paulot, F. and Jacob, D. J.: Hidden Cost of U.S. Agricultural Exports: Particulate Matter from Ammonia Emissions, *Environ. Sci. Technol.*, 48, 903–908, <https://doi.org/10.1021/es4034793>, 2014.
- Paulot, F., Jacob, D. J., Johnson, M. T., Bell, T. G., Baker, A. R., Keene, W. C., Lima, I. D., Doney, S. C., and Stock, C. A.: Global oceanic emission of ammonia: Constraints from seawater and atmospheric observations, *Global Biogeochem. Cy.*, 29, 1165–1178, <https://doi.org/10.1002/2015GB005106>, 2015.
- Paulot, F., Ginoux, P., Cooke, W. F., Donner, L. J., Fan, S., Lin, M.-Y., Mao, J., Naik, V., and Horowitz, L. W.: Sensitivity of nitrate aerosols to ammonia emissions and to nitrate chemistry: implications for present and future nitrate optical depth, *Atmos. Chem. Phys.*, 16, 1459–1477, <https://doi.org/10.5194/acp-16-1459-2016>, 2016.
- Paulot, F., Paynter, D., Ginoux, P., Naik, V., Whitburn, S., Van Damme, M., Clarisse, L., Coheur, P.-F., and Horowitz, L.: Gas-aerosol partitioning of ammonia in biomass burning plumes: Implications for the interpretation of spaceborne observations of ammonia and the radiative forcing of ammonium nitrate, *Geophys. Res. Lett.*, 44, 8084–8093, <https://doi.org/10.1002/2017GL074215>, 2017.
- Perrino, C., Catrambone, M., Di Bucchianico, A. D. M., and Allegrini, I.: Gaseous ammonia in the urban area of Rome, Italy and its relationship with traffic emissions, *Atmos. Environ.*, 36, 5385–5394, [https://doi.org/10.1016/S1352-2310\(02\)00469-7](https://doi.org/10.1016/S1352-2310(02)00469-7), 2002.
- Pinder, R., Gilliland, A., and Dennis, R.: Environmental impact of atmospheric NH₃ emissions under present and future conditions in the eastern United States, *Geophys. Res. Lett.*, 35, L12808, <https://doi.org/10.1029/2008GL033732>, 2008.
- Pinder, R. W., Pekney, N. J., Davidson, C. I., and Adams, P. J.: A process-based model of ammonia emissions from dairy cows: improved temporal and spatial resolution, *Atmos. Environ.*, 38, 1357–1365, <https://doi.org/10.1016/j.atmosenv.2003.11.024>, 2004a.
- Pinder, R. W., Strader, R., Davidson, C. I., and Adams, P. J.: A temporally and spatially resolved ammonia emission inventory for dairy cows in the United States, *Atmos. Environ.*, 38, 3747–3756, <https://doi.org/10.1016/j.atmosenv.2004.04.008>, 2004b.
- Pinder, R. W., Adams, P. J., Pandis, S. N., and Gilliland, A. B.: Temporally resolved ammonia emission inventories: Current estimates, evaluation tools, and measurement needs, *J. Geophys. Res.-Atmos.*, 111, D16310, <https://doi.org/10.1029/2005JD006603>, 2006.
- Pinder, R. W., Adams, P. J., and Pandis, S. N.: Ammonia emission controls as a cost-effective strategy for reducing atmospheric particulate matter in the eastern United States, *Environ. Sci. Technol.*, 41, 380–386, <https://doi.org/10.1021/es060379a>, 2007.
- Pleim, J. E., Bash, J. O., Walker, J. T., and Cooter, E. J.: Development and evaluation of an ammonia bidirectional flux parameterization for air quality models, *J. Geophys. Res.-Atmos.*, 118, 3794–3806, <https://doi.org/10.1002/jgrd.50262>, 2013.
- Poulain, L., Spindler, G., Birmili, W., Plass-Dülmer, C., Wiedensohler, A., and Herrmann, H.: Seasonal and diurnal variations of particulate nitrate and organic matter at the IfT research station Melpitz, *Atmos. Chem. Phys.*, 11, 12579–12599, <https://doi.org/10.5194/acp-11-12579-2011>, 2011.
- Pozzer, A., Tsimpidi, A. P., Karydis, V. A., de Meij, A., and Lelieveld, J.: Impact of agricultural emission reductions on fine-particulate matter and public health, *Atmos. Chem. Phys.*, 17, 12813–12826, <https://doi.org/10.5194/acp-17-12813-2017>, 2017.
- Reche, C., Viana, M., Karanasiou, A., Cusack, M., Alastuey, A., Artiñano, B., Revuelta, M. A., López-Mahía, P., Blanco-Heras, G., Rodríguez, S., Sánchez de la Campa, A. M., Fernández-Camacho, R., González-Castanedo, Y., Mantilla, E., Sim Tanh, Y., and Querol, X.: Urban NH₃ levels and sources in six major Spanish cities, *Chemosphere*, 119, 769–777, <https://doi.org/10.1016/j.chemosphere.2014.07.097>, 2015.
- Rittmann, B. E. and McCarty, P. L.: *Environmental biotechnology: principles and applications*, McGraw-Hill, New York, NY, 2001.
- Robarge, W. P., Walker, J. T., McCulloch, R. B., and Murray, G.: Atmospheric concentrations of ammonia and ammonium at an agricultural site in the southeast United States, *Atmos. Environ.*, 36, 1661–1674, [https://doi.org/10.1016/S1352-2310\(02\)00171-1](https://doi.org/10.1016/S1352-2310(02)00171-1), 2002.
- Schmohl, A., Miklos, A., and Hess, P.: Effects of adsorption-desorption processes on the response time and accuracy of photoacoustic detection of ammonia, *Appl. Opt.*, 40, 2571–2578, <https://doi.org/10.1364/AO.40.002571>, 2001.
- Seinfeld, J. H. and Pandis, S. N.: *Atmospheric chemistry and physics: from air pollution to climate change*, John Wiley & Sons, Hoboken, NJ, 2016.
- Sickles, J. E. and Shadwick, D. S.: Comparison of particulate sulfate and nitrate at collocated CASTNET and IMPROVE

- sites in the eastern US, *Atmos. Environ.*, 42, 2062–2073, <https://doi.org/10.1016/j.atmosenv.2007.11.051>, 2008.
- Siefert, R. L., Scudlark, J. R., Potter, A. G., Simonsen, K. A., and Savidge, K. B.: Characterization of atmospheric ammonia emissions from a commercial chicken house on the Delmarva Peninsula, *Environ. Sci. Technol.*, 38, 2769–2778, <https://doi.org/10.1021/es0345874>, 2004.
- Sorooshian, A., Murphy, S. M., Hersey, S., Gates, H., Padro, L. T., Nenes, A., Brechtel, F. J., Jonsson, H., Flagan, R. C., and Seinfeld, J. H.: Comprehensive airborne characterization of aerosol from a major bovine source, *Atmos. Chem. Phys.*, 8, 5489–5520, <https://doi.org/10.5194/acp-8-5489-2008>, 2008.
- Stein, A., Draxler, R. R., Rolph, G. D., Stunder, B. J., Cohen, M., and Ngan, F.: NOAA's HYSPLIT atmospheric transport and dispersion modeling system, *B. Am. Meteorol. Soc.*, 96, 2059–2077, <https://doi.org/10.1175/BAMS-D-14-00110.1>, 2015.
- Stelson, A. and Seinfeld, J. H.: Relative humidity and temperature dependence of the ammonium nitrate dissociation constant, *Atmos. Environ.*, 16, 983–992, [https://doi.org/10.1016/0004-6981\(82\)90184-6](https://doi.org/10.1016/0004-6981(82)90184-6), 1982.
- Stull, R. B.: *An Introduction to Boundary Layer Meteorology*, vol. 13, Springer Science & Business Media, the Netherlands, 1988.
- Sullivan, J. T., Berkoff, T., Gronoff, G., Knepp, T., Pippin, M., Allen, D., Twigg, L., Swap, R., Tzortziou, M., Thompson, A. M., Stauffer, R. M., Wolfe, G. M., Flynn, J., Pusede, S. E., Judd, L. M., Moore, W., Baker, B. D., Al-Saadi, J., and McGee, T. J.: The Ozone Water–Land Environmental Transition Study: An Innovative Strategy for Understanding Chesapeake Bay Pollution Events, *B. Am. Meteorol. Soc.*, 100, 291–306, <https://doi.org/10.1175/BAMS-D-18-0025.1>, 2019.
- Sun, K., Tao, L., Miller, D. J., Pan, D., Golston, L. M., Zondlo, M. A., Griffin, R. J., Wallace, H. W., Leong, Y. J., Yang, M. M., Zhang, Y., Mauzerall, D. L., and Zhu, T.: Vehicle Emissions as an Important Urban Ammonia Source in the United States and China, *Environ. Sci. Technol.*, 51, 2472–2481, <https://doi.org/10.1021/acs.est.6b02805>, 2017.
- Sutton, M., Dragosits, U., Tang, Y., and Fowler, D.: Ammonia emissions from non-agricultural sources in the UK, *Atmos. Environ.*, 34, 855–869, [https://doi.org/10.1016/S1352-2310\(99\)00362-3](https://doi.org/10.1016/S1352-2310(99)00362-3), 2000.
- Sutton, M. A., Reis, S., Riddick, S. N., Dragosits, U., Nemitz, E., Theobald, M. R., Tang, Y. S., Braban, C. F., Vieno, M., Dore, A. J., Mitchell, R. F., Wanless, S., Daunt, F., Fowler, D., Blackall, T. D., Milford, C., Flechard, C. R., Loubet, B., Massad, R., Cellier, P., Personne, E., Coheur, P. F., Clarisse, L., Van Damme, M., Ngadi, Y., Clerbaux, C., Skjøth, C. A., Geels, C., Hertel, O., Wichink Kruit, R. J., Pinder, R. W., Bash, J. O., Walker, J. T., Simpson, D., Horváth, L., Misselbrook, T. H., Bleeker, A., Dentener, F., and de Vries, W.: Towards a climate-dependent paradigm of ammonia emission and deposition, *Philos. T. Roy. Soc. B*, 368, 1–13, <https://doi.org/10.1098/rstb.2013.0166>, 2013.
- Tsigaridis, K., Daskalakis, N., Kanakidou, M., Adams, P. J., Artaxo, P., Bahadur, R., Balkanski, Y., Bauer, S. E., Bellouin, N., Benedetti, A., Bergman, T., Berntsen, T. K., Beukes, J. P., Bian, H., Carslaw, K. S., Chin, M., Curci, G., Diehl, T., Easter, R. C., Ghan, S. J., Gong, S. L., Hodzic, A., Hoyle, C. R., Iversen, T., Jathar, S., Jimenez, J. L., Kaiser, J. W., Kirkevåg, A., Koch, D., Kokkola, H., Lee, Y. H., Lin, G., Liu, X., Luo, G., Ma, X., Mann, G. W., Mihalopoulos, N., Morcrette, J.-J., Müller, J.-F., Myhre, G., Myriokefalitakis, S., Ng, N. L., O'Donnell, D., Penner, J. E., Pozzoli, L., Pringle, K. J., Russell, L. M., Schulz, M., Sciare, J., Seland, Ø., Shindell, D. T., Sillman, S., Skeie, R. B., Spracklen, D., Stavrou, T., Steenrod, S. D., Takemura, T., Tittita, P., Tilmes, S., Tost, H., van Noije, T., van Zyl, P. G., von Salzen, K., Yu, F., Wang, Z., Wang, Z., Zaveri, R. A., Zhang, H., Zhang, K., Zhang, Q., and Zhang, X.: The AeroCom evaluation and intercomparison of organic aerosol in global models, *Atmos. Chem. Phys.*, 14, 10845–10895, <https://doi.org/10.5194/acp-14-10845-2014>, 2014.
- Turnock, S., Mann, G., Woodhouse, M., Dalvi, M., O'Connor, F., Carslaw, K., and Spracklen, D.: The impact of changes in cloud water pH on aerosol radiative forcing, *Geophys. Res. Lett.*, 46, 4039–4048, <https://doi.org/10.1029/2019GL082067>, 2019.
- USDA: Census of Agriculture, Volume 1, chap. 2, County Level Data, United States Department of Agriculture, Tech. rep., 2017.
- Valerino, M., Johnson, J., Izumi, J., Orozco, D., Hoff, R., Delgado, R., and Hennigan, C.: Sources and composition of PM_{2.5} in the Colorado Front Range during the DISCOVER-AQ study, *J. Geophys. Res.-Atmos.*, 122, 566–582, <https://doi.org/10.1002/2016JD025830>, 2017.
- Van Damme, M., Clarisse, L., Whitburn, S., Hadji-Lazaro, J., Hurtmans, D., Clerbaux, C., and Coheur, P.-F.: Industrial and agricultural ammonia point sources exposed, *Nature*, 564, 99–103, <https://doi.org/10.1038/s41586-018-0747-1>, 2018.
- von Bobruzki, K., Braban, C. F., Famulari, D., Jones, S. K., Blackall, T., Smith, T. E. L., Blom, M., Coe, H., Gallagher, M., Ghaliyeny, M., McGillen, M. R., Percival, C. J., Whitehead, J. D., Ellis, R., Murphy, J., Mohacsi, A., Pogany, A., Junninen, H., Rantanen, S., Sutton, M. A., and Nemitz, E.: Field inter-comparison of eleven atmospheric ammonia measurement techniques, *Atmos. Meas. Tech.*, 3, 91–112, <https://doi.org/10.5194/amt-3-91-2010>, 2010.
- Vutukuru, S. and Dabdub, D.: Modeling the effects of ship emissions on coastal air quality: A case study of southern California, *Atmos. Environ.*, 42, 3751–3764, <https://doi.org/10.1016/j.atmosenv.2007.12.073>, 2008.
- Warner, J., Dickerson, R., Wei, Z., Stow, L. L., Wang, Y., and Liang, Q.: Increased atmospheric ammonia over the world's major agricultural areas detected from space, *Geophys. Res. Lett.*, 44, 2875–2884, <https://doi.org/10.1002/2016GL072305>, 2017.
- Washenfelder, R. A., Attwood, A. R., Brock, C. A., Guo, H., Xu, L., Weber, R. J., Ng, N. L., Allen, H. M., Ayres, B. R., Baumann, K., Cohen, R. C., Draper, D. C., Duffey, K. C., Edger-ton, E., Fry, J. L., Hu, W. W., Jimenez, J. L., Palm, B. B., Romer, P., Stone, E. A., Wooldridge, P. J., and Brown, S. S.: Biomass burning dominates brown carbon absorption in the rural southeastern United States, *Geophys. Res. Lett.*, 42, 653–664, <https://doi.org/10.1002/2014GL062444>, 2015.
- Weber, R.: Short-term temporal variation in PM_{2.5} mass and chemical composition during the Atlanta Super-site Experiment, 1999, *J. Air Waste Manage.*, 53, 84–91, <https://doi.org/10.1080/10473289.2003.10466123>, 2003.
- Weber, R. J., Guo, H., Russell, A. G., and Nenes, A.: High aerosol acidity despite declining atmospheric sulfate concentrations over the past 15 years, *Nat. Geosci.*, 9, 282–285, <https://doi.org/10.1038/ngeo2665>, 2016.

- Wittig, A. E., Anderson, N., Khlystov, A. Y., Pandis, S. N., Davidson, C., and Robinson, A. L.: Pittsburgh air quality study overview, *Atmos. Environ.*, 38, 3107–3125, <https://doi.org/10.1016/j.atmosenv.2004.03.003>, 2004.
- Wolfe, G.: HYSPLITcontrol, GitHub [code], <https://github.com/AirChem/HYSPLITcontrol>, last access: 28 July 2021.
- Wyers, G., Otjes, R., and Slanina, J.: A continuous-flow denuder for the measurement of ambient concentrations and surface-exchange fluxes of ammonia, *Atmos. Environ.*, 27, 2085–2090, [https://doi.org/10.1016/0960-1686\(93\)90280-C](https://doi.org/10.1016/0960-1686(93)90280-C), 1993.
- Xu, L., Suresh, S., Guo, H., Weber, R. J., and Ng, N. L.: Aerosol characterization over the southeastern United States using high-resolution aerosol mass spectrometry: spatial and seasonal variation of aerosol composition and sources with a focus on organic nitrates, *Atmos. Chem. Phys.*, 15, 7307–7336, <https://doi.org/10.5194/acp-15-7307-2015>, 2015.
- Fu, X., Wang, T., Zhang, L., Li, Q., Wang, Z., Xia, M., Yun, H., Wang, W., Yu, C., Yue, D., Zhou, Y., Zheng, J., and Han, R.: The significant contribution of HONO to secondary pollutants during a severe winter pollution event in southern China, *Atmos. Chem. Phys.*, 19, 1–14, <https://doi.org/10.5194/acp-19-1-2019>, 2019.
- Zhao, B., Wang, S., Wang, J., Fu, J. S., Liu, T., Xu, J., Fu, X., and Hao, J.: Impact of national NO_x and SO₂ control policies on particulate matter pollution in China, *Atmos. Environ.*, 77, 453–463, <https://doi.org/10.1016/j.atmosenv.2013.05.012>, 2013.
- Zhu, L., Henze, D., Bash, J., Jeong, G.-R., Cady-Pereira, K., Shephard, M., Luo, M., Paulot, F., and Capps, S.: Global evaluation of ammonia bidirectional exchange and livestock diurnal variation schemes, *Atmos. Chem. Phys.*, 15, 12823–12843, <https://doi.org/10.5194/acp-15-12823-2015>, 2015.